

GFlowNet-EM for Learning Compositional Latent Variable Models

Edward J. Hu^{*1} Nikolay Malkin^{*1} Moksh Jain¹ Katie Everett^{2,3} Alexandros Graikos⁴ Yoshua Bengio^{1,5}

Abstract

Latent variable models (LVMs) with discrete compositional latents are an important but challenging setting due to a combinatorially large number of possible configurations of the latents. A key tradeoff in modeling the posteriors over latents is between expressivity and tractable optimization. For algorithms based on expectation-maximization (EM), the E-step is often intractable without restrictive approximations to the posterior. We propose the use of GFlowNets, algorithms for sampling from an unnormalized density by learning a stochastic policy for sequential construction of samples, for this intractable E-step. By training GFlowNets to sample from the posterior over latents, we take advantage of their strengths as amortized variational inference algorithms for complex distributions over discrete structures. Our approach, GFlowNet-EM, enables the training of expressive LVMs with discrete compositional latents, as shown by experiments on non-context-free grammar induction and on images using discrete variational autoencoders (VAEs) without conditional independence enforced in the encoder.

Code: github.com/GFNORG/GFlowNet-EM.

1. Introduction

In the real world, we often observe high-dimensional data that is generated from lower-dimensional latent variables (Bishop, 2006). In particular, it is often natural for these latent variables to have a discrete, compositional structure for data domains like images and language. For example, an image might be decomposed into individual objects that have a relationship between their positions, and natural language utterances contain individual words that describe

^{*}Equal contribution ¹Mila, Université de Montréal ²Google Research ³Massachusetts Institute of Technology ⁴Stony Brook University ⁵CIFAR Fellow. Correspondence to: Edward J. Hu <edward@edwardjhu.com>.

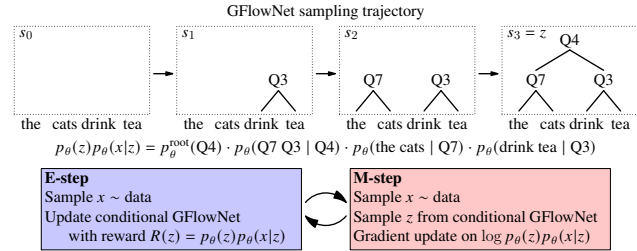


Figure 1. GFlowNet-EM for training a latent variable model $p_\theta(z)p_\theta(x|z)$ to maximize likelihood of observed data x . The generative model here is a probabilistic context-free grammar. The GFlowNet samples a latent parse tree z from an approximation to the posterior $p_\theta(z|x)$. GFlowNet-EM can flexibly handle non-context-free grammars, black-box priors on tree shape, etc. (§5.2).

relationships between abstract concepts. Modeling this discrete compositional latent structure allows for combining existing concepts in new ways, an important inductive bias for human-like generalization (Goyal & Bengio, 2022).

One family of approaches for maximum-likelihood estimation in LVMs is based on the expectation-maximization algorithm (EM; Dempster et al., 1977), which we review in §2.1. However, inference of the posterior over latent variables, which is needed in the E-step of EM, is generally intractable when there are combinatorially large number of possible configurations for the latents, such as when the latent random variable does not factorize and represents a discrete compositional structure like a tree or graph. One can approximately sample from this posterior by running Markov Chain Monte Carlo (MCMC), which can be prohibitively expensive and suffer from poor mixing properties. Another approach is to impose conditional independence assumptions on the generative model or on the posterior approximation; the latter is known as variational EM (see §2.1). Both limit the expressivity of the LVM. One such example studied here is the induction of context-free grammars (Baker, 1979), which has a generative model under which the expansion of a symbol is independent of its context.

Generative flow networks (GFlowNets; Bengio et al., 2021; 2023), which we review in §2.2, are an amortized inference method for sampling from unnormalized densities by sequentially constructing samples using a learned stochastic

policy. This sequential construction makes GFlowNets especially useful for sampling discrete compositional objects like trees or graphs. In this work, we propose to use GFlowNets to learn an amortized sampler of the intractable posterior conditioned on a data sample (Fig. 1). This enables the learning of LVMs without conditional independence assumptions, or with weaker ones compared to traditional LVMs like probabilistic context-free grammars (PCFGs). We also make several algorithmic contributions to mitigate the optimization challenges in jointly learning a GFlowNet sampler and a generative model, notably, posterior collapse (Wang et al., 2021), when the learned posterior only models a few of the modes of the true posterior. We validate our method, which we call GFlowNet-EM, on both language and image domains. We intend for this work to serve as a tool for learning more powerful latent variable models that were previously prohibitively expensive to learn.

Our contributions include:

- (1) The GFlowNet-EM framework for maximum likelihood estimation in discrete compositional LVMs that are intractable to optimize by exact EM;
- (2) Algorithmic improvements to stabilize joint learning with the generative model while mitigating posterior collapse;
- (3) Empirical demonstrations of LVMs with intractable posteriors learned with GFlowNet-EM, including a non-context-free grammar and a discrete VAE without independence assumptions in the encoder.

2. Background

2.1. Expectation-Maximization (EM)

We review the standard formulation of the EM algorithm (Dempster et al., 1977) and its variational form (Neal & Hinton, 1998; Koller & Friedman, 2009). Consider a LVM with a directed graphical model structured as $z \rightarrow x$, with likelihood given by $p(x) = \sum_z p_\theta(z)p_\theta(x|z)$. The latent z may itself have hierarchical structure and be generated through a sequence of intermediate latent variables. Given a dataset $\{x^i\}_{i=1}^T$, we wish to optimize the parameters θ to maximize the data log-likelihood

$$\mathcal{L} = \log \prod_{i=1}^T p(x^i) = \sum_{i=1}^T \log \sum_z p_\theta(z)p_\theta(x^i|z). \quad (1)$$

The EM algorithm achieves this by maximizing a variational bound on Eq. 1, known as the evidence lower bound (ELBO)

or negative free energy:

$$\begin{aligned} \mathcal{L} &\geq \sum_{i=1}^T \mathbb{E}_{z \sim q(z|x^i)} \log \frac{p_\theta(z)p_\theta(x^i|z)}{q(z|x^i)} \\ &= \mathcal{L} - \sum_{i=1}^T D_{\text{KL}}(q(z|x^i) \| p(z|x^i)), \end{aligned} \quad (2)$$

where $p(z|x^i) \propto p_\theta(z)p_\theta(x^i|z)$ is the true posterior over the latent. The inequality holds for any collection of distributions $q(z|x^i)$ and is an equality if and only if q equals the true posterior.

An important choice in EM algorithms is how to parameterize and store the distributions $q(z|x^i)$. In simple EM applications like mixture models, they are stored in a tabular way, i.e., as a matrix of logits that represents the true posterior (*exact EM*). In other settings, q is constrained to lie in a simpler family of distributions, and this family need not contain the true posterior (*variational EM*). A common simplifying assumption is one of conditional independence between components of z , e.g., if $z = (z_1, z_2, z_3)$, then $q(z|x^i) = q(z_1|x^i)q(z_2|x^i)q(z_3|x^i)$ (see §3). Finally, in *amortized variational EM*, $q(z|x^i)$ can be parametrized as a neural network, as we will describe below.

The EM algorithm iterates two steps, each of which increases the ELBO (Eq. 2):

E-step. Optimize the distributions $q(z|x^i)$ so as to approximately make $q(z|x^i) \propto p_\theta(z)p_\theta(x^i|z)$. If q , or its factors, are stored in a tabular way, this step is as simple as appropriately normalizing the full matrix $p_\theta(z)p_\theta(x^i|z)$. In other applications, such as for fitting VAEs, q can be optimized using gradient steps to minimize $D_{\text{KL}}(q(z|x^i) \| p(z|x^i))$.

M-step. Optimize \mathcal{L} with respect to the parameters of p , as by taking gradient steps on

$$\mathbb{E}_i[\mathbb{E}_{z \sim q(z|x^i)} \log p_\theta(z)p_\theta(x^i|z)]. \quad (3)$$

Amortized variational EM. In amortized variational EM, q is parametrized by a neural network q_ϕ taking x^i as input, which allows evaluation of $q_\phi(z|x)$ at any x and thus generalization to unseen data: sampling from $q(-|x^i)$ becomes easy, at the amortized cost of having to train the neural net. The ELBO can also be jointly optimized with respect to the parameters of both q and p instead of through separate E and M steps. This is the principle behind VAE models (Rezende et al., 2014; Kingma & Welling, 2014).

Wake-sleep for EM. We return to the question of the E-step – optimizing q – when q is parametrized as a neural network $q_\phi(z|x)$. To maximize the ELBO (Eq. 2), q needs to be trained to minimize $D_{\text{KL}}(q(z|x^i) \| p(z|x^i))$ for data

samples x^i .¹ If z is high-dimensional, this network can be difficult to train and q_ϕ may not assign high likelihood to all modes of the true posterior (*posterior collapse*): when a mode is not represented in q , no sample from that mode is ever drawn, which would make it impossible to update q to represent that mode. Instead, q tends to focus on a single mode, even if it can in principle represent multiple modes.

The *sleep phase*, a procedure originally used for fitting posteriors over latents in deep stochastic networks (Hinton et al., 1995) but later generalized to other settings (Bornschein & Bengio, 2015; Le et al., 2019; Hewitt et al., 2020), aims to mitigate posterior collapse. In the sleep phase, latents $z \sim p_\theta(z)$ and data $x \sim p_\theta(x|z)$ are hallucinated from the generative model (‘dreamt’, as opposed to ‘wakeful’ use of real data x^i), and $q_\phi(z|x)$ is optimized with respect to its likelihood of recovering z . That is, the objective minimizes

$$\mathbb{E}_{z \sim p_\theta(z), x \sim p_\theta(x|z)} [-\log q_\phi(z|x)]. \quad (4)$$

For a given x , this objective is equivalent to minimizing $D_{\text{KL}}(p_\theta(z|x) \| q_\phi(z|x))$, the opposite direction of the KL compared to Eq. 2. This direction of the KL will cause q_ϕ to seek a broad approximation to the true posterior that captures all of its modes, preventing posterior collapse. On the other hand, if hallucinated samples x are not close to the distribution of the real data x^i , the sleep phase may not provide a useful gradient signal for the posteriors $q_\phi(z|x^i)$ that are used in the M-step Eq. 3 with real x^i . Therefore, both wake and sleep E-steps can be combined in practice (Bornschein & Bengio, 2015; Le et al., 2019).

2.2. GFlowNets

We briefly review GFlowNets and their training objectives. For a broader introduction, the reader is directed to Malkin et al. (2022), whose conventions and notation we borrow, and to other papers listed in §6.1.

GFlowNets (Bengio et al., 2021) are a family of algorithms for training a stochastic policy to sample objects from a target distribution over a set of objects \mathcal{Z} (such as complete parse trees, in Fig. 1). The set \mathcal{Z} is a subset of a larger *state space* \mathcal{S} , which contains partially constructed objects (like the incomplete parse trees in the first three panels of Fig. 1). Formally, the state space has the structure of a directed acyclic graph, where vertices are *states* and edges are *actions* that transition from one state to another. There is a designated *initial state* s_0 with no parents (incoming edges), while the *terminal states* – those with no children (outgoing edges) – are in bijection with the complete objects \mathcal{Z} . A *complete trajectory* is a sequence of states $s_0 \rightarrow s_1 \rightarrow \dots \rightarrow s_n = z$, where $x \in \mathcal{Z}$ and each $s_i \rightarrow s_{i+1}$ is an action (like an addition of a node to the parse tree).

¹Such training can not be done directly in general, since the true posterior is unknown, but algorithms, including GFlowNet-EM, use the fact that $p(z|x^i) \propto p_\theta(z)p_\theta(x^i|z)$, which is available.

A (*forward*) *policy* is a collection of distributions $P_F(s'|s)$ over the children of every nonterminal state $s \in \mathcal{S} \setminus \mathcal{Z}$. A policy induces a distribution over complete trajectories $\tau = (s_0 \rightarrow \dots \rightarrow s_n)$ given by $P_F(\tau) = \prod_{i=1}^n P_F(s_i|s_{i-1})$. This distribution can be sampled by starting at s_0 and sequentially sampling actions from P_F to reach the next state. The policy P_F also induces a distribution P_F^\top over the terminal states via

$$P_F^\top(z) = \sum_{\tau \text{ leading to } z} P_F(\tau). \quad (5)$$

That is, $P_F^\top(z)$ is the marginal likelihood that a trajectory sampled from P_F terminates at z .

Training GFlowNets. Given a reward function $R : \mathcal{Z} \rightarrow \mathbb{R}_{\geq 0}$, the goal of GFlowNets is to learn a parametric policy $P_F(s'|s; \theta)$ such that $P_F^\top(z) \propto R(z)$, i.e., the policy samples an object with likelihood proportional to its reward. Because P_F^\top is a (possibly intractable) sum over trajectories (5), auxiliary quantities need to be introduced to optimize for reward-proportional sampling. The most commonly used objective in recent work, trajectory balance (TB; Malkin et al., 2022), requires learning two models in addition to the forward policy: a *backward policy* $P_B(s|s'; \theta)$, which is a distribution over the *parents* of every noninitial state, and a scalar Z_θ , which is an estimate of the partition function (total reward). The TB objective for a trajectory $\tau = (s_0 \rightarrow \dots \rightarrow s_n = z)$ is

$$\mathcal{L}_{\text{TB}}(\tau; \theta) = \left[\log \frac{Z_\theta \prod_{i=1}^n P_F(s_i|s_{i-1}; \theta)}{R(z) \prod_{i=1}^n P_B(s_{i-1}|s_i; \theta)} \right]^2. \quad (6)$$

If this loss is made equal to 0 for all trajectories τ , then the policy $P_F(-|s)$ samples proportionally to the reward. (From now on, we omit the dependence of P_F , P_B , and Z on θ for simplicity.)

In practice, this loss can be minimized by gradient descent on θ for trajectories sampled either *on-policy*, taking $\tau \sim P_F(\tau)$ from the current version of the policy, or *off-policy*. Just as in reinforcement learning (RL), off-policy training can be done in various ways, such as by sampling τ from a tempered version $P_F^\#$ of the current policy or by sampling $\tau \sim P_B(\tau|z)$ from the *backward* policy starting at a known terminal state. Madan et al. (2023) introduce subtrajectory balance (SubTB), which generalizes TB to partial trajectories.

Conditional GFlowNets. GFlowNets can be conditioned on other variables (Bengio et al., 2023; Jain et al., 2022b; Zhang et al., 2023b). If the reward depends on a variable x , then the learned models P_F , P_B , and Z can all take x as an input and be trained to sample from the conditional reward $R(z|x)$. GFlowNet-EM makes critical use of this ability to model the posterior conditioned on a given data sample.

3. Motivating Example: Pitfalls of Factorization

To illustrate the drawbacks of a factorized posterior, we consider a hierarchical version of a Gaussian mixture model as a toy example. The data is generated from a set of superclusters, in which each supercluster has a set of subclusters, which we call ‘petals’ because each is located at a fixed offset around the supercluster mean as in Fig. 3. The data generation process first selects which supercluster, then which petal subcluster, a point should be sampled from, and then samples the point from a standard normal distribution centered at the component mean that is determined by the supercluster mean μ_i plus the appropriate offset for the selected petal j . This problem illustrates a setting where the true posterior $p(i, j|x)$ has a dependence between the discrete latent factors i and j , where i denotes the supercluster and j denotes the petal subcluster.

We consider a small version of this problem with four supercluster means arranged in a grid shape where each supercluster has four petals. We use a fixed variance and uniform priors over the choice of supercluster and petal for each data point. The model must learn only the positions of the supercluster means so as to maximize the data likelihood.

This arrangement induces multiple modes in the true posterior $p(i, j|x)$ for a particular estimate of the supercluster means μ ; for example, there can be ambiguity about whether a certain point came from the top left petal of one supercluster or the top right petal of another supercluster (Fig. 2). This requires the inference algorithm to perform combinatorial reasoning to infer optimal assignments (i.e., considering all (i, j) combinations), which is a notoriously difficult problem for algorithms that use a mean-field posterior approximation.

In this problem, we can easily perform the exact E-step by modeling the posterior in a tabular fashion, where $q(i, j|x)$ is computed exactly as a categorical distribution over all possible pairs (i, j) . However, if we were to increase the number of levels of the hierarchy, with each point explained by a combination of many more than two factors, computing the exact posterior would become intractable.

Meanwhile, *factorized* posteriors can be computed analytically for generative models with this structure (Ghahramani, 1994). To alleviate the scalability limitations as the depth of the hierarchy grows, we could perform variational EM using the mean-field assumption, so that the approximate posterior is factorized as $q(i, j|x) = q(i|x)q(j|x)$ and a separate categorical distribution is modeled over each latent factor. Yet, as seen in Fig. 2 the factorized approximation fails to assign the proper posterior, and as shown with Fig. 3, EM with a factorized approximation to the posterior fails to recover the true supercluster means even on this small dataset.

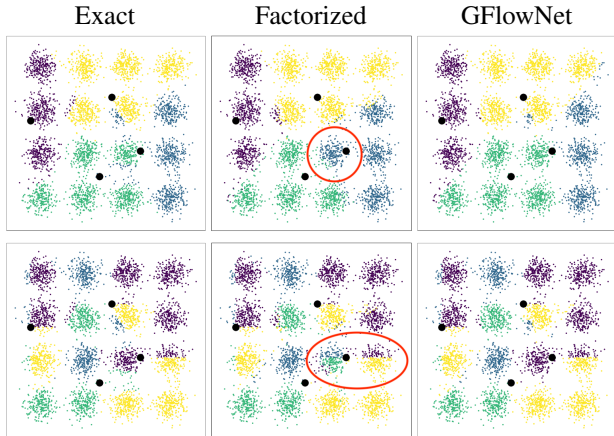


Figure 2. Posteriors $q(i, j|x)$ inferred during a single E-step for a particular estimate of supercluster means (black dots). **Top row:** colour indicates which *supercluster* (value of i) each point is assigned to. **Bottom row:** colour indicates which *petal* (value of j) each point is assigned to. Assignments use the most likely pair (i, j) for each point in the posterior $q(i, j|x)$. Note the different behaviour of the factorized posterior in the areas circled in red.

This simple example illustrates the fundamental limitations of factorized posteriors. In more complicated problems, e.g., models for layer separation in computer vision (Frey & Jojic, 2005), this effect can become more pronounced.

In contrast, the posterior learned by GFlowNet-EM, which makes no independence assumptions on the approximate posterior, achieves a better fit to the true posterior while being more scalable. We elaborate on this approach in the next section.

4. GFlowNet-EM

The GFlowNet-EM algorithm simultaneously trains two models: the generative model $p_\theta(z, x)$, factorized as $p_\theta(z)p_\theta(x|z)$, and a conditional GFlowNet $q(z|x) = P_F^T(z|x)$ that approximates the true posterior $p_\theta(z|x)$.

E-step. The GFlowNet is conditioned on x and trained to sample z with reward $R(z|x) = p_\theta(z)p_\theta(x|z)$. If trained perfectly, the GFlowNet’s marginal terminating distribution $P_F^T(z|x)$ – note the dependence of P_F on the conditioning variable x – is proportional to $R(z|x)$, and thus the policy $P_F(-|-, x)$ samples from the true posterior.

In the problems we study, z is a discrete compositional object, and a state space needs to be designed to enable sequential construction of z by a GFlowNet policy. We describe the state space for each setting in our experiments in the corresponding section (Section 5).

Algorithm 1 GFlowNet-EM: Basic form with thresholding

Require: Data $\{x^i\}$, generative model with parameters θ , GFlowNet with parameters ϕ , optimization and exploration hyperparameters, threshold α

- 1: **repeat**
- 2: Sample $x^i \sim \text{data}$
- 3: Sample $\tau \sim P_F^\#(\tau|x^i)$; $z \leftarrow$ (last state of τ)
- 4: $\mathcal{L} \leftarrow$ [TB loss along τ with reward $p_\theta(z)p_\theta(x|z)$]
- 5: E-step: gradient update on ϕ with $\nabla_\phi \mathcal{L}$
- 6: **if** $\mathcal{L} < \alpha$ **then**
- 7: Sample $\tau \sim P_F(\tau|x^i)$; $z \leftarrow$ (last state of τ)
- 8: M-step: gradient update on θ with $\nabla_\theta [-\log p_\theta(z)p_\theta(x|z)]$
- 9: **end if**
- 10: **until** some convergence condition

M-step. The terminating distribution $P_F^\top(z|x)$ of the GFlowNet is used as a variational approximation to the posterior to perform updates to the generative model’s parameters. Namely, for a data sample x^i , we sample a terminal state – a latent z – from the policy of the conditional GFlowNet and perform a gradient update on $\log p_\theta(z)p_\theta(x^i|z)$, thus performing in expectation a gradient update on (3).

Note that because the generative model p_θ evolves over the course of joint optimization, the reward for the GFlowNet is nonstationary. E-steps and M-steps are alternated in the course of training, and the schedule of gradient updates – number of GFlowNet updates in between successive M-steps – is a parameter that can be fixed or chosen adaptively. We discuss the challenges arising from joint training, and solutions to them, in Section 4.1.

The basic form of the algorithm, including an adaptive E-step schedule, is presented as Algorithm 1.

4.1. GFlowNet-EM Optimization Techniques

GFlowNet-EM presents two challenges that are not present in standard GFlowNet training. First, the estimated posterior $q(z|x)$ is conditioned on the data point x , and the dependence of the reward function on x may be complex. Second, the GFlowNet is trained with a nonstationary reward, as the generative model p , which provides the reward, changes over the course of GFlowNet-EM training. On the other hand, it is important for the GFlowNet to track the true posterior as it evolves, so as not to bias the M-step and produce degenerate solutions. We employ a variety of new and existing techniques to address these two challenges. The existing techniques are reviewed in Appendix A. Ablation studies are presented in §C.7 and §5.3 to demonstrate the effectiveness of individual techniques.

Algorithm 2 GFlowNet-EM: E-step (sleep phase)

- 1: Sample $z \sim p_\theta(z), x \sim p_\theta(x|z)$
- 2: Sample trajectory $\tau \sim P_B(\tau|z, x)$ leading to z
- 3: Gradient step on ϕ with $\nabla_\phi [-\log P_F(\tau|x)]$

Adaptive E-steps via loss thresholding. If the GFlowNet were able to model the true posterior perfectly, one could reduce the GFlowNet loss to zero after every M-step (yielding exact EM). This is, however, unrealistic due to finite model capacity and compute constraints. We propose a method for adaptively choosing the number of updates to the GFlowNet that are performed in between successive M-step gradient updates. Treating a moving average of the GFlowNet’s training loss as an indicator of how well the true posterior is approximated, we heuristically set a loss *threshold*, and perform an M-step gradient update after an update to the GFlowNet only if this moving average falls below the threshold. A lower threshold corresponds to requiring a more accurate approximate posterior for updating the generative model. Because the posterior tends to become simpler to model during the course of training from a random initialization, we use a heuristic threshold schedule that linearly decreases the requisite threshold to trigger an M-step update.

Local credit assignment with modular log-likelihood.

In some interesting LVMS, such as those in §5.2, the reward decomposes as a product of terms accumulated over steps of the sampling sequence. In this case, a forward-looking SubTB loss as described in Pan et al. (2023) can be used as the GFlowNet objective instead of TB.

Exploratory training policy. Off-policy exploration in GFlowNet training can be used to improve mode coverage. The ability of GFlowNets to be stably trained off-policy is a key strength compared to other variational inference algorithms (Malkin et al., 2023). As described in §5, we employ two exploration methods: *policy tempering* (making $P_F^\#(s'|s, x)$ proportional to $P_F(s'|s, x)^\beta$ for some $\beta < 1$) and *ϵ -uniform sampling* (making $P_F^\#(s'|s, x)$ a mixture of $P_F(s'|s, x)$ and a uniform distribution over the action space).

4.2. Improving Posterior Estimation

A sleep phase for GFlowNet-EM. We propose adding a sleep phase to the E-step updates of GFlowNet-EM, taking advantage of the ability to sample ancestrally from the generative model to prevent posterior collapse.

The sleep phase requires minimizing $-\log q(z|x)$ as in Eq. 4 for z, x sampled ancestrally from the generative model. However, $q(z|x) = P_F^\top(z|x)$ is a (possibly intractable) sum of likelihoods of all sampling trajectories leading to z . To

optimize this log-likelihood, we sample a trajectory leading to z from the *backward* policy $\tau \sim P_B(\tau|z, x)$ and optimize the parameters of the *forward* policy P_F with objective $-\log P_F(\tau|x)$. This amounts to maximizing the log-likelihood that the GFlowNet’s sampling policy conditioned on x recovers z by following the sampling trajectory τ . It can be shown that for any fixed value of the parameters of P_B , the global optimum of this objective with respect to P_F is a maximizer of $\log P_F^\top(z|x)$, guaranteeing correctness. Theoretical results and experiments related to this maximum likelihood training objective for GFlowNets can be found in Zhang et al. (2023a).

MCMC using GFlowNet as the proposal distribution.

Another way to leverage the generative model to better estimate the posterior is to run a short MCMC chain initialized with samples drawn from the GFlowNet to bring them closer to the true posterior distribution. The MCMC proposal can make use of the GFlowNet policy itself, using the ‘back-and-forth’ proposal of Zhang et al. (2022).

5. Empirical Results

5.1. Hierarchical Mixture Revisited

As our first experiment, we compare exact EM, variational EM with a factorized posterior, and GFlowNet-EM on the hierarchical mixture dataset presented in §3. For GFlowNet-EM, the E-step is performed by a GFlowNet conditioned on the data. The GFlowNet’s policy, parametrized as a small MLP, takes two actions: the first action chooses the supercluster assignment and the second action chooses the petal assignment. The reward can be set to $R(i, j|x) = p(x|i, j)$, proportional to the posterior $p(i, j|x)$ as the prior $p(i, j)$ is uniform.

Averaged over twenty random seeds, after sixty iterations (which induces convergence in all methods), the data log-likelihood per sample for exact EM is -5.79 ± 0.74 , variational EM is -7.26 ± 1.12 , and GFlowNet-EM is -5.77 ± 0.48 . For reference, the average log-likelihood for the ground truth supercluster means, used to sample the dataset, is -5.62 ± 0.01 . Implementation details are described in Appendix B. The estimated supercluster means for each method on a single initialization are shown in Fig. 3, where exact EM and GFlowNet-EM both nearly match the ground truth supercluster means but variational EM fails to learn the correct means.

5.2. Grammar Induction on Penn Tree Bank (PTB)

In linguistics and in the theory of formal languages, a grammar refers to a set of structure constraints on sequences of symbols. Since Chomsky (1965), all dominant theories have assumed some form of hierarchical generative grammar as a

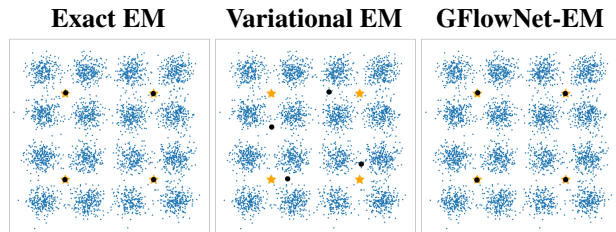


Figure 3. Estimated supercluster means are shown as black dots while ground truth supercluster means are shown as orange stars. Unlike the (factorized) Variational EM, GFlowNet-EM puts the means at the right place.

universal feature of natural languages. The task of grammar induction asks whether one can automatically discover from data the *hierarchical* grammar that explains the *sequential* structure we observe, and whether the discovered rules coincide with ones created by human experts. We study the case with binary rule branching. See §C.1 for a more detailed description of the assumptions we make on the grammar and the way the rule likelihoods are parametrized.

Dataset. We use a subset of Penn Tree Bank (PTB; Marcus et al., 1999) that contains sentences with 20 or fewer tokens. Otherwise, we follow the preprocessing done by Kim et al. (2019), including removing punctuation and tokenizing OOV words. The vocabulary size (number of T symbols) is 9672. We use 30 NT symbols and 60 PT symbols.

Baselines. We reproduce the Neural PCFG architecture from Kim et al. (2019). Taking advantage of specialized algorithms for context-free grammars, we either marginalize over the latent space (*Marginalization*²) or sample from the true posterior (*Exact sampling EM*). Our *Marginalization* baseline matches the result produced by the public repository of Kim et al. (2019). The Monte-Carlo EM (MC-EM) baseline draws samples from the posterior by running 1000 MCMC steps with a proposal distribution that performs random single tree rotations and symbol changes. All baseline and GFlowNet-EM runs are run for 10,000 grammar (M-step) gradient updates. We use Torch-Struct (Rush, 2020) to perform marginalization and exact sampling in PCFGs.

Metrics. We use two metrics to evaluate learned grammars:

- (1) The marginal likelihood of a held-out dataset under the learned grammar, which can be equivalently expressed in terms of negative log-likelihood per word. When marginalization is not tractable, we use a variational upper bound described in §C.5.

²The marginal likelihood has the same gradient as exact sampling EM in expectation.

Table 1. Inducing a context-free grammar (CFG) or a non-context-free-grammar (Non-CFG) using different methods. GFlowNet-EM allows the incorporation of an energy-based model (EBM) prior or the use of an intractable grammar, e.g., Non-CFG. All configuration are run over 5 random seeds.

Grammar	Method	NLL / word ↓	Sentence F1 ↑
CFG	Marginalization	5.61 ± 0.01	39.51 ± 7.01
	Exact-sampling EM	5.74 ± 0.05	31.17 ± 6.06
	MC-EM	5.88 ± 0.01	22.31 ± 1.04
	+ EBM Prior	5.91 ± 0.02	23.81 ± 1.41
	GFlowNet-EM + EBM Prior	5.70 ± 0.03 5.79 ± 0.03	34.85 ± 3.39 48.41 ± 1.38
Non-CFG	MC-EM	-	18.98 ± 0.26
	GFlowNet-EM	≤ 5.46 ± 0.07	38.68 ± 1.90

(2) How well the parse trees under the learned grammar resemble human-labeled trees, as measured by an F1 score between sets of spans (constituents) in a proposed and a human-labeled parse tree, following Kim et al. (2019). This metric evaluates the linguistic relevance of the learned grammar.

GFlowNet-EM parametrization. The GFlowNet models the posterior over possible parse trees given a sentence (a sequence of Ts, i.e., terminal symbols). Even though we only consider binary trees, following Kim et al. (2019), the number of possible trees is exponential both in the sequence length and in the number of PTs and NTs.³ We propose a bottom-up GFlowNet action space, which incrementally joins two adjacent partial trees by hanging them under a common parent, as illustrated in Fig. 1. The initial state is represented by the sequence of n terminal symbols x , each of which is a tree of depth zero. A binary parse tree is obtained after $n - 1$ joining steps. We only generate the NT symbols in the tree and marginalize over PT symbols, as this can be done in linear time (see §C.3). We use a Transformer (Vaswani et al., 2017) with full attention over root nodes and a bottom-up MLP aggregator; see §C.2 for more details and §C.7 for ablations studying the different components of GFlowNet-EM.

In addition to the basic algorithm in Alg. 1, we use a forward-looking SubTB loss, a sleep phase (Alg. 2), and MCMC steps as described in §4.1 for the grammar induction experiment.

5.2.1. CONTEXT-FREE GRAMMAR

We first consider the well-studied problem of inducing a binary branching probabilistic context-free grammar (PCFG), where the rule probabilities are independent of the context. In this case, the true posterior over parse trees is tractable to

³Even the number of binary tree *shapes* for a sequence of length n is the Catalan number $\frac{1}{n} \binom{2(n-1)}{n-1} = O(4^n / n\sqrt{n})$.

sample from or even marginalize over using an algorithm with run time cubic in the sequence length (Baker, 1979). Nonetheless, we validate GFlowNet-EM by comparing it with exact EM, i.e., always sampling from the exact posterior. As *Exact sampling EM* is equivalent to GFlowNet-EM with the constraint that the GFlowNet is perfectly trained to zero loss on every E-step, the exact sampling baseline gives a rough upper bound on the performance of GFlowNet-EM without additional inductive biases.

Results. *Marginalization* baseline performs the best in terms of both NLL and F1, as shown in Table 1, which we attribute to its much lower gradient variance compared to drawing samples from the true posterior. GFlowNet-EM can match and exceed sampling from the exact posterior on both metrics, despite having to learn an approximate posterior sampler. It is worth noting that while GFlowNet-EM is not necessary in this scenario, it has an asymptotic computational advantage because it amortizes the cost of inference; see §C.6 for more details.

We now consider setups where *Marginalization* and *Exact sampling* are not tractable.

5.2.2. CFG WITH ENERGY-BASED MODEL GUIDANCE

It can be useful to bias learned LVMs to incorporate domain-specific knowledge. For example, we might want the learned grammar to produce parse trees that have shapes resembling ones provided by human annotators for linguistic interest. This preference for tree shapes is hard to integrate because it is a global attribute, which violates the strong conditional independence assumptions in CFGs that are required for correctness of exact sampling algorithms.

We train an energy-based model (EBM) on the *shapes* of human-labeled trees to represent black-box domain knowledge. The EBM’s density acts as a prior that is multiplied by the usual GFlowNet reward. We anneal the temperature of this prior to infinity in 10,000 steps, thus only biasing the beginning (symmetry-breaking) phase of the joint learning process. See more details in §C.4.

Results. Table 1 shows that GFlowNet-EM with the EBM prior can learn grammars that produce trees more similar to human annotation compared to *Exact sampling EM* and even *Marginalization*. We also note that the trees generated have a strong right-branching bias, a well-known feature of English syntax.

5.2.3. NON-CONTEXT-FREE GRAMMAR

The context-free assumption in CFGs makes exact sampling from the posterior tractable. GFlowNet-EM, however, does not require the true posterior to be tractable, as long as there is underlying structure for amortized learning. To this end,

we experiment with a non-context-free grammar (Non-CFG) that allows a rule probability to depend on the parent of the LHS of the rule (§C.5), for which exact sampling from the posterior over parse trees becomes prohibitively expensive.

Results. As shown in Table 1, GFlowNet-EM on this Non-CFG yields a grammar that has a significantly lower marginal NLL while having a comparable F1 to *Marginalization* on a CFG, despite drawing finite samples from a learned approximate posterior. This is attributed to the more expressive generative model and to inductive biases of its parametrization: we do not incorporate any external knowledge, e.g., an EBM prior, in this experiment.

5.3. Discrete Variational Autoencoders

Next, we study the problem of learning deep generative models of images with discrete latent representations. This problem was previously posed under the framework of vector-quantized variational autoencoders (VQ-VAE; van den Oord et al., 2017). VQ-VAEs assume a latent space of the form $\{1, \dots, K\}^n$, where n is the length of the latent vector and K is the number of possible values for each position. However, the VQ-VAE decoder represents each value in $\{1, \dots, K\}$ by its representation vector in a vector space \mathbb{R}^D , while the encoder predicts a vector in \mathbb{R}^D and maps it to the value in $\{1, \dots, K\}$ whose representation vector is nearest to the prediction. This manner of passing through a high-dimensional continuous space allows passing approximate gradients from the decoder to the encoder using the straight-through estimator (Bengio et al., 2013), but is inherently incapable of learning more than a single-point estimate of the posterior over discrete latents.

GFlowNet encoder. We propose to use a GFlowNet as the encoder to learn a policy that sequentially constructs the discrete latent representation of an image (Fig. 4). The E-step trains the encoder model to match the posterior distribution over the discrete latents z conditioned on an image x , and the M-step trains the decoder to minimize the error in reconstructing x from the latent sampled by the encoder.

Crucially, this approach does not rely on an approximation of gradients, as the E and M steps are decoupled, and admits an expressive posterior by imposing none of the conditional independence constraints on components of the latent that VAE encoders make. Furthermore, VQ-VAEs assume a uniform prior over the discrete latents z . However, GFlowNet-EM enables us to also learn a prior distribution, $p_\theta(z)$, jointly with the decoder $p_\theta(x|z)$. This is a clear advantage over VQ-VAEs, which can only learn the prior distribution post-hoc, after the encoder is trained.

We chose an autoregressive encoder: it sequentially constructs the discrete latent by sampling one categorical entry at a

Table 2. GFlowNet-EM achieves lower NLL than VQ-VAE on the static MNIST test set (mean and std. over 5 runs; GFlowNet NLL estimated using 5000 importance-weighted samples). **Bold:** the lowest NLL and all those not significantly higher than it ($p > 0.1$ under an unpaired t -test).

Method	Codebook size		
	$K = 4$	$K = 8$	$K = 10$
VQ-VAE	86.36 \pm 0.14	80.84 \pm 0.39	82.96 \pm 0.38
GFlowNet-EM	74.18 \pm 0.41	70.74 \pm 0.99	70.67 \pm 0.72
+ Greedy Decoder Training (GD)	76.22 \pm 0.58	72.03 \pm 0.98	72.69 \pm 1.56
+ GD + Jointly Learned Prior	78.59 \pm 1.48	70.84 \pm 1.06	71.69 \pm 1.90

time, conditioned on the input image and the previously drawn entries (Fig. 4). This reduces the complexity of the encoder network while maintaining an advantage over VQ-VAEs, where the posterior is fully factorized.

For these experiments we modify Alg. 1 by (i) not using an adaptive E-step, but alternately performing 400 E-steps and 400 M-steps and (ii) using sleep phase exploration (Alg. 2).

Training and evaluation. To train the encoder and decoder networks, we alternate between E- and M-steps, using 400 gradient updates in each step (see §D for details). We found that this was adequate and no adaptive E-step was needed. During E-steps, we exploit the sleep phase for exploration, where we sample z from either the uniform or learned prior and x from the current $p_\theta(x|z)$. We also observe that convergence is accelerated by training the decoder with samples drawn *greedily* from the learned encoder policy, although this gives a biased objective in the M-step and results in slightly lower test data likelihood.

Results and discussion. We perform our experiments on the static MNIST dataset (Deng, 2012), with a 4×4 spatial latent representation and using dictionaries of sizes $K \in \{4, 8, 10\}$ and dimensionality $D = 1$. We compare with a VQ-VAE with the same latent representation as a baseline. (For codebook sizes larger than 10, we observed the NLL of the VQ-VAE increase.) In Table 2 we show estimated NLL on the test set obtained by the VQ-VAE model and different variations of GFlowNet-EM for all dictionary sizes K . In all experiments, GFlowNet-EM performs significantly better than VQ-VAE, which we attribute to the higher expressiveness of the posterior.

Just as for VQ-VAEs, decoded samples with the latent drawn from a uniform prior do not resemble real images. When the prior $p(z)$ is also learned jointly with $p(x|z)$, we achieve similar results to those assuming a uniform prior, but also gain the ability to draw reasonable unconditional samples from the prior (Fig. 6).

We note that the more expressive posterior and lower NLL come with an increased training cost. Sampling from the

posterior requires multiple forward passes of the GFlowNet encoder, and performing the E and M steps alternately entails more training iterations than are needed for VQ-VAEs.

6. Related Work

6.1. GFlowNets

GFlowNets (Bengio et al., 2021; 2023) were first formulated as a reinforcement learning algorithm that generalizes maximum-entropy RL (Haarnoja et al., 2018) to settings with multiple paths to the same state. However, recent papers (Malkin et al., 2023; Zimmermann et al., 2022; Zhang et al., 2023a) place GFlowNets in the family of variational methods, showing that they are more amenable to stable off-policy training than policy gradient approaches to minimizing divergences between distributions. Applications include biological molecule and sequence design (Jain et al., 2022a;b), causal structure learning (Deleu et al., 2022; Nishikawa-Toomey et al., 2022), and robust combinatorial optimization (Zhang et al., 2023b). Energy-based GFlowNets (Zhang et al., 2022) solve the related problem of fitting a GFlowNet to a nonstationary reward defined by a generative model from which exact sampling is intractable; however, the updates to the generative model are approximate contrastive divergence steps, and inference over latent variables is not performed. GFlowNets were also used as approximate posteriors for an ELBO maximization in Liu et al. (2022).

6.2. Latent Variable Models and EM

Discrete LVMs, prominent before the deep learning revolution, continue to motivate research, including on posterior regularization techniques (Ganchev et al., 2010), theoretical properties of EM (Neath et al., 2013), augmenting classical latent variable models with distributed neural representations (Dieng et al., 2020), adapting discrete LVMs to deep learning-scale data for robust classification (Malkin et al., 2020), and amortized inference (Agrawal & Domke, 2021).

6.3. Applications

Grammar induction. The literature on automatic grammar induction, briefly described in §5.2, is most focused on probabilistic context-free grammars and their variants, thanks to the efficient learning algorithm introduced in Baker (1979) and Lari & Young (1990). Many variants have increased the expressivity of PCFGs without relaxing the context-free assumption, such as Kim et al. (2019) and Zhao & Titov (2021). While the learning of PCFGs can be accelerated with careful implementations (Yang et al., 2021; Rush, 2020), their time complexity remains cubic in the length of the sequences and in the number of NT and PT symbols. PCFG induction has been applied to

character-level multilingual language modeling (Jin et al., 2021) and music modeling with the addition of continuous symbols (Lieck & Rohrmeier, 2021).

Discrete VAEs. Discrete latent representations, as popularized by VQ-VAEs (van den Oord et al., 2017), have been shown to successfully capture both abstract and low-level features (Esser et al., 2021; Baevski et al., 2020; Dhariwal et al., 2020). In comparison to their continuous VAE counterparts (Kingma & Welling, 2014), discrete latent variable models utilize more efficiently the available latent degrees of freedom due to their inherent ability to ignore imperceptible input details. The main limitations of discrete VAE models arise from their use of a continuous relaxation to allow for backpropagation (Ramesh et al., 2021) and the fundamental limitation of having to learn the prior over the latent variable separately. GFlowNet-EM overcomes both of these limitations.

7. Conclusions

We presented a novel method for maximum-likelihood estimation in discrete latent variable models that uses GFlowNets as approximate samplers of the posterior for intractable E-steps. Our experiments on non-context-free grammar induction and discrete image representations – both settings where the LVM has an intractable posterior without additional independence assumptions – show that GFlowNet-EM outperforms existing approaches. Future work should broaden the applications of GFlowNet-EM to other compositional latent variable models, particularly those with continuous or hybrid latents.

Acknowledgements

The authors thank Matt Hoffman, Tuan Anh Le, Donna Vakalis, and the anonymous ICML reviewers for their comments on drafts of the paper, as well as Nebojsa Jojic, Paul Soulos, and Dinghuai Zhang for some helpful discussions. They are also grateful for the financial support from IBM, Samsung, Microsoft and Google.

References

- Agrawal, A. and Domke, J. Amortized variational inference for simple hierarchical models. *Neural Information Processing Systems (NeurIPS)*, 2021.
- Baevski, A., Zhou, Y., Mohamed, A., and Auli, M. wav2vec 2.0: A framework for self-supervised learning of speech representations. *Neural Information Processing Systems (NeurIPS)*, 2020.
- Baker, J. K. Trainable grammars for speech recognition.

- The Journal of the Acoustical Society of America*, 65(S1): S132–S132, 1979.
- Bengio, E., Jain, M., Korablyov, M., Precup, D., and Bengio, Y. Flow network based generative models for non-iterative diverse candidate generation. *Neural Information Processing Systems (NeurIPS)*, 2021.
- Bengio, Y., Léonard, N., and Courville, A. C. Estimating or propagating gradients through stochastic neurons for conditional computation. *arXiv preprint 1308.3432*, 2013.
- Bengio, Y., Lahlou, S., Deleu, T., Hu, E., Tiwari, M., and Bengio, E. GFlowNet foundations. *Journal of Machine Learning Research (JMLR)*, 2023. To appear.
- Bishop, C. M. *Pattern Recognition and Machine Learning*. Springer, 2006.
- Bornschein, J. and Bengio, Y. Reweighted wake-sleep. *International Conference on Learning Representations (ICLR)*, 2015.
- Chomsky, N. *Aspects of the Theory of Syntax*. MIT Press, 1965.
- Deleu, T., Góis, A., Emezue, C., Rankawat, M., Lacoste-Julien, S., Bauer, S., and Bengio, Y. Bayesian structure learning with generative flow networks. *Uncertainty in Artificial Intelligence (UAI)*, 2022.
- Dempster, A. P., Laird, N. M., and Rubin, D. B. Maximum likelihood from incomplete data via the EM algorithm. *Journal of the Royal Statistical Society B*, 39(1):1–38, 1977.
- Deng, L. The MNIST database of handwritten digit images for machine learning research. *IEEE Signal Processing Magazine*, 29(6):141–142, 2012.
- Dhariwal, P., Jun, H., Payne, C., Kim, J. W., Radford, A., and Sutskever, I. Jukebox: A generative model for music. *arXiv preprint 2005.00341*, 2020.
- Dieng, A. B., Ruiz, F. J. R., and Blei, D. M. Topic modeling in embedding spaces. *Transactions of the Association for Computational Linguistics*, 8:439–453, 2020. doi: 10.1162/tacl.a.00325. URL <https://aclanthology.org/2020.tacl-1.29>.
- Esser, P., Rombach, R., and Ommer, B. Taming transformers for high-resolution image synthesis. *Computer Vision and Pattern Recognition (CVPR)*, 2021.
- Frey, B. and Jojic, N. A comparison of algorithms for inference and learning in probabilistic graphical models. *IEEE Transactions on Pattern Analysis and Machine Intelligence*, 27(9):1392–1416, 2005.
- Ganchev, K., Graça, J., Gillenwater, J., and Taskar, B. Posterior regularization for structured latent variable models. *Journal of Machine Learning Research (JMLR)*, 11: 2001–2049, aug 2010.
- Ghahramani, Z. Factorial learning and the EM algorithm. *Neural Information Processing Systems (NIPS)*, 1994.
- Goyal, A. and Bengio, Y. Inductive biases for deep learning of higher-level cognition. *Proceedings of the Royal Society A*, 478(2266):20210068, 2022.
- Haarnoja, T., Zhou, A., Abbeel, P., and Levine, S. Soft actor-critic: Off-policy maximum entropy deep reinforcement learning with a stochastic actor. *International Conference on Machine Learning (ICML)*, 2018.
- Hewitt, L. B., Le, T. A., and Tenenbaum, J. B. Learning to learn generative programs with memoised wake-sleep. *Uncertainty in Artificial Intelligence (UAI)*, 2020.
- Hinton, G. E., Dayan, P., Frey, B. J., and Neal, R. M. The “wake-sleep” algorithm for unsupervised neural networks. *Science*, 268 5214:1158–61, 1995.
- Jain, M., Bengio, E., Hernandez-Garcia, A., Rector-Brooks, J., Dossou, B. F., Ekbote, C., Fu, J., Zhang, T., Kilgour, M., Zhang, D., Simine, L., Das, P., and Bengio, Y. Biological sequence design with GFlowNets. *International Conference on Machine Learning (ICML)*, 2022a.
- Jain, M., Raparthy, S. C., Hernandez-Garcia, A., Rector-Brooks, J., Bengio, Y., Miret, S., and Bengio, E. Multi-objective GFlowNets. *arXiv preprint 2210.12765*, 2022b.
- Jin, L., Oh, B.-D., and Schuler, W. Character-based PCFG induction for modeling the syntactic acquisition of morphologically rich languages. In *Findings of the Association for Computational Linguistics: EMNLP 2021*, pp. 4367–4378, Punta Cana, Dominican Republic, November 2021. Association for Computational Linguistics. doi: 10.18653/v1/2021.findings-emnlp.371. URL <https://aclanthology.org/2021.findings-emnlp.371>.
- Kim, Y., Dyer, C., and Rush, A. Compound probabilistic context-free grammars for grammar induction. In *Proceedings of the 57th Annual Meeting of the Association for Computational Linguistics*, pp. 2369–2385, Florence, Italy, July 2019. Association for Computational Linguistics. doi: 10.18653/v1/P19-1228. URL <https://aclanthology.org/P19-1228>.
- Kingma, D. P. and Welling, M. Auto-encoding variational Bayes. *International Conference on Learning Representations (ICLR)*, 2014.

- Koller, D. and Friedman, N. *Probabilistic graphical models: principles and techniques*. MIT press, 2009.
- Lari, K. and Young, S. The estimation of stochastic context-free grammars using the inside-outside algorithm. *Computer Speech and Language*, 4(1):35–56, 1990.
- Le, T. A., Kosiorek, A. R., Siddharth, N., Teh, Y. W., and Wood, F. Revisiting reweighted wake-sleep for models with stochastic control flow. *Neural Information Processing Systems (NeurIPS)*, 2019.
- Lieck, R. and Rohrmeier, M. Recursive Bayesian networks: Generalising and unifying probabilistic context-free grammars and dynamic Bayesian networks. *Neural Information Processing Systems (NeurIPS)*, 2021.
- Liu, D., Jain, M., Dossou, B. F. P., Shen, Q., Lahlou, S., Goyal, A., Malkin, N., Emezue, C. C., Zhang, D., Hassen, N., Ji, X., Kawaguchi, K., and Bengio, Y. GFlowOut: Dropout with generative flow networks. *arXiv preprint 2210.12928*, 2022.
- Madan, K., Rector-Brooks, J., Korablyov, M., Bengio, E., Jain, M., Nica, A., Bosc, T., Bengio, Y., and Malkin, N. Learning GFlowNets from partial episodes for improved convergence and stability. *International Conference on Machine Learning (ICML)*, 2023.
- Malkin, N., Ortiz, A., and Jovic, N. Mining self-similarity: Label super-resolution with epitomic representations. *European Conference on Computer Vision (ECCV)*, 2020.
- Malkin, N., Jain, M., Bengio, E., Sun, C., and Bengio, Y. Trajectory balance: Improved credit assignment in GFlowNets. *Neural Information Processing Systems (NeurIPS)*, 2022.
- Malkin, N., Lahlou, S., Deleu, T., Ji, X., Hu, E., Everett, K., Zhang, D., and Bengio, Y. GFlowNets and variational inference. *International Conference on Learning Representations (ICLR)*, 2023.
- Marcus, M. P., Santorini, B., Marcinkiewicz, M. A., and Taylor, A. Treebank-3. *Linguistic Data Consortium, Philadelphia*, 14, 1999.
- Neal, R. M. and Hinton, G. E. A view of the em algorithm that justifies incremental, sparse, and other variants. In *Learning in graphical models*, pp. 355–368. Springer, 1998.
- Neath, R. C. et al. On convergence properties of the Monte Carlo EM algorithm. *Advances in modern statistical theory and applications: a Festschrift in Honor of Morris L. Eaton*, pp. 43–62, 2013.
- Nishikawa-Toomey, M., Deleu, T., Subramanian, J., Bengio, Y., and Charlin, L. Bayesian learning of causal structure and mechanisms with GFlowNets and variational bayes. *arXiv preprint 2211.02763*, 2022.
- Pan, L., Malkin, N., Zhang, D., and Bengio, Y. Better training of GFlowNets with local credit and incomplete trajectories. *International Conference on Machine Learning (ICML)*, 2023.
- Ramesh, A., Pavlov, M., Goh, G., Gray, S., Voss, C., Radford, A., Chen, M., and Sutskever, I. Zero-shot text-to-image generation. *International Conference on Machine Learning (ICML)*, 2021.
- Rezende, D. J., Mohamed, S., and Wierstra, D. Stochastic backpropagation and approximate inference in deep generative models. *International Conference on Machine Learning (ICML)*, 2014.
- Rush, A. Torch-struct: Deep structured prediction library. In *Proceedings of the 58th Annual Meeting of the Association for Computational Linguistics: System Demonstrations*, pp. 335–342, Online, July 2020. Association for Computational Linguistics. doi: 10.18653/v1/2020.acl-demos.38. URL <https://aclanthology.org/2020.acl-demos.38>.
- van den Oord, A., Kalchbrenner, N., and Kavukcuoglu, K. Pixel recurrent neural networks. *International Conference on Machine Learning (ICML)*, 2016.
- van den Oord, A., Vinyals, O., and Kavukcuoglu, K. Neural discrete representation learning. *Neural Information Processing Systems (NIPS)*, 2017.
- Vaswani, A., Shazeer, N., Parmar, N., Uszkoreit, J., Jones, L., Gomez, A. N., Kaiser, L., and Polosukhin, I. Attention is all you need. *Neural Information Processing Systems (NIPS)*, 2017.
- Wang, Y., Blei, D. M., and Cunningham, J. P. Posterior collapse and latent variable non-identifiability. *Neural Information Processing Systems (NeurIPS)*, 2021.
- Yang, S., Zhao, Y., and Tu, K. PCFGs can do better: Inducing probabilistic context-free grammars with many symbols. In *Proceedings of the 2021 Conference of the North American Chapter of the Association for Computational Linguistics: Human Language Technologies*, pp. 1487–1498, Online, June 2021. Association for Computational Linguistics. doi: 10.18653/v1/2021.naacl-main.117. URL <https://aclanthology.org/2021.naacl-main.117>.
- Zhang, D., Malkin, N., Liu, Z., Volokhova, A., Courville, A., and Bengio, Y. Generative flow networks for discrete probabilistic modeling. *International Conference on Machine Learning (ICML)*, 2022.

Zhang, D., Chen, R. T. Q., Malkin, N., and Bengio, Y. Unifying generative models with GFlowNets and beyond. *arXiv preprint 2209.02606v2*, 2023a.

Zhang, D., Rainone, C., Peschl, M., and Bondesan, R. Robust scheduling with GFlowNets. *International Conference on Learning Representations (ICLR)*, 2023b.

Zhao, Y. and Titov, I. An empirical study of compound PCFGs. In *Proceedings of the Second Workshop on Domain Adaptation for NLP*, pp. 166–171, Kyiv, Ukraine, April 2021. Association for Computational Linguistics. URL <https://aclanthology.org/2021.adaptnlp-1.17>.

Zimmermann, H., Lindsten, F., van de Meent, J.-W., and Naesseth, C. A. A variational perspective on generative flow networks. *arXiv preprint 2210.07992*, 2022.

A. On GFlowNet optimization techniques

For the sake of completeness, we review the SubTB loss from Madan et al. (2023) and the forward-looking parametrization from Pan et al. (2023).

Subtrajectory balance (SubTB). In addition to the forward and backward policy models $P_F(s'|s)$ and $P_B(s|s')$, one trains a state flow estimator $F(s)$, which outputs a scalar for any state in the GFlowNet state space. If $\tau = (s_0 \rightarrow \dots \rightarrow s_n)$ is a complete trajectory and $\tau_{i:j} = (s_i \rightarrow s_{i+1} \rightarrow \dots \rightarrow s_j)$ is its subtrajectory, the SubTB loss $\tau_{i:j}$ is defined as

$$\mathcal{L}_{\text{SubTB}}(\tau_{i:j}) = \frac{F(s_i)P_F(s_{i+1}|s_i)P_F(s_{i+2}|s_{i+1}) \dots P_F(s_j|s_{j-1})}{F(s_j)P_B(s_i|s_{i+1})P_B(s_{i+1}|s_{i+2}) \dots P_B(s_{j-1}|s_j)},$$

where we enforce $F(s) = R(s)$ if s is terminal. Thus $\mathcal{L}_{\text{SubTB}}$ reduces to the TB loss if s_i is initial and s_j is terminal, where $F(s_0)$ is identified with Z .

The SubTB objective for a complete trajectory $\tau = (s_0 \rightarrow \dots \rightarrow s_n)$ with $\lambda = 1$, as defined in Madan et al. (2023), is the average of SubTB losses for all of its partial trajectories:

$$\mathcal{L}(\tau) = \frac{1}{\binom{n+1}{2}} \sum_{0 \leq i < j \leq n} \mathcal{L}_{\text{SubTB}}(\tau_{i:j}).$$

Forward-looking loss. The state flow estimator $F(s)$ used in SubTB is typically parametrized in the log domain, i.e., a neural network taking s as input outputs $\log F(s)$. In the case where one has available a *partial reward* accumulated up to state s – denoted $\tilde{R}(s)$ – the forward-looking parametrization from Pan et al. (2023) parametrizes $\log F(s) = \log \tilde{R}(s) + g(s; \theta)$, where g is a neural network.

Note that \tilde{R} can be an arbitrary estimate of the negative ‘partial energy’ of a state s , and $\tilde{R} \equiv 0$ yields the regular SubTB objective. However, natural partial log-rewards exist in cases where the low-reward is close to additive over steps taken in a trajectory. For example, in the case of a parser for a context-free grammar, if s is a partially constructed tree, we take $\log \tilde{R}(s)$ to be the sum of log-likelihoods under the grammar of the production rules that occur in s .

B. Hierarchical mixture

This section describes the experiment setup for the hierarchical mixture experiments in §5.1. We sample 20 datasets and one initialization of the supercluster means per dataset, where the initial supercluster means are selected to be random points from the data. For each dataset and initialization, we run exact EM, variational EM, and GFlowNet-EM and compute the log-likelihood under the the estimated supercluster means after the final iteration. We run all methods for 60 iterations, which induces convergence in all methods.

The GFlowNet takes 1000 gradient steps in each E-step, samples one latent assignment per data point from the posterior, and takes one gradient step in each M-step. Note that such an optimization method is chosen simply for illustration; the objective in the M-step is quadratic in the parameters and can be optimized in closed form, a case of a more general algorithm for Gaussian multiple cause models (Ghahramani, 1994).

We implemented several of the optimization techniques in §4.1 (loss thresholding and epsilon-uniform sampling), but the empirical impacts are negligible on this problem as the basic GFlowNet-EM method easily matches the optimal solution found by exact EM.

C. Grammar induction

C.1. Experiment setup

In our setup, following Kim et al. (2019), there are 30 NT symbols and 60 PT symbols in addition to T symbols. In addition, among these NT symbols is a special root symbol, which we call ROOT, that is fixed to be the root of each parse tree. For convenience, we shall use NT to refer to non-terminal symbols that are not the special ROOT token. The root symbol has only one child, which is allowed to be any NT symbols, i.e., $\text{ROOT} \rightarrow \text{NT}$. There are $|NT|$, i.e., number of NT symbols, such rules. Each NT symbol is allowed to branch in two symbols, each belonging to the union of all NT and PT symbols,

Table 3. Hyperparameters for training the GFlowNet-EM for grammar induction.

Hyperparameter	Value
Encoder Transformer: Layers	6
Hidden Dimension	512
Adam β	(0.9, 0.99)
Batch Size	32
P_F, P_B : Learning Rate	10^{-4}
Z: Learning Rate	0.03
MCMC Step	10
Sleep phase weight	10
SubTB λ	1
EBM Prior temperature start	1
EBM Prior temperature end	1000
EBM Prior temperature schedule horizon	10000
Adaptive threshold max	6
Adaptive threshold min	3
Adaptive threshold schedule horizon	10000
Grammar: MLP Hidden Dimension	256
Grammar: Learning Rate	0.001
Grammar: Adam β	(0.75, 0.999)

i.e., $NT \rightarrow \{NT, PT\} \{NT, PT\}$. There are $|NT|^3|PT|^2$ such rules. Finally, each PT symbol is allowed to turn into a T symbol, i.e., a vocabulary item. There are $|PT||V|$ such rules of the form $PT \rightarrow V$, where $|V|$ is the size of the vocabulary.

A naive parametrization would use a table to store individual rule probabilities without assuming any dependencies among them. This, however, is not conducive to learning expressive and linguistically meaningful grammars as described in Kim et al. (2019). Kim et al. (2019) propose a distributed representation, where each symbol is assigned an embedding and rule probabilities are computed using an MLP. See the Neural PCFG in Kim et al. (2019) for the specifics of this grammar parametrization.

C.2. GFlowNet parametrization

Given an input x represented as a sequence of tokens, we would like to sample a parse tree z according to $p(z|x)$. We construct the parse tree z bottom-up as illustrated in Fig. 1. The state space of the GFlowNet is the space of ordered forests, where a tree represents a sub-tree in the final z . The action space is all pairs of adjacent trees in an ordered forest. At every time step, we choose one such pair and join them with a new parent to form a new tree. We use a Transformer (Vaswani et al., 2017) with full attention, which processes only the root nodes of trees in the ordered forest. The information from non-root nodes are encoded using an aggregator. For every binary branching, we recursively compute the embedding of the parent node using the static embedding for the symbol at that node combined with the recursively computed embeddings of its children using an MLP. The embeddings of root nodes, which now encode whole trees, are passed to the Transformer encoder. The policies P_F and P_B and the flow estimator F are implemented as MLP heads on top of the Transformer encoder. We use a sum-pooling operation for the flow estimator, which gives a scalar for every GFlowNet state regardless of how many trees it contains.

Training hyperparameters are listed in Table 3.

C.3. Marginalizing preterminals

The construction of a parse tree z given a sentence x is conventionally done in two steps: 1) tagging and 2) parsing. The tagging step assigns each terminal (T) symbol a preterminal (PT) symbol, and the parsing steps join nonterminal (NT) symbols and PT symbols alike using NT symbols. Using a GFlowNet to tag T symbols doubles the number of time steps it needs to construct z for a sentence. This is especially wasteful considering that tagging step can be easily marginalized over in linear time. As a result, we use the GFlowNet to join T symbols directly and produce parse trees without any PT symbols.

Table 4. Hyperparameters for training the EBM prior on tree shapes.

Hyperparameter	Value
MLP Hidden Dimension	16
Learning Rate	10^{-5}
Adam β	(0.9, 0.99)
L_2 Regularization	10^{-4}
Batch Size	32
Sequence Length	40

When evaluating the reward of such trees, we perform a marginalization over all PT symbols in each position, which can be done in linear time for both the context-free grammar and the non-context-free grammar we introduced.

C.4. Training energy-based model prior

In §5.2.2, we use an energy-based model (EBM) as a prior on tree shapes. This EBM is trained with a persistent contrastive divergence objective on gold trees from the training set, where the MCMC proposal used in PCD is a random tree rotation (i.e., replacement of a random subtree of the form $[X[YZ]]$ by $[[XY]Z]$ or vice versa) and the buffer reset ratio is 0.1. The EBM architecture was a recursive aggregator similar to that described in Appendix C.2: the embedding of a node is a MLP evaluated on a concatenation of the embeddings of its children, the embeddings of leaf nodes are fixed to zero vectors, and the output energy is a pooled embedding of the root. This ensures that the energy depends only on the tree *shape* and not on the symbols. The hyperparameter for training the EBM are listed in Table 4. To make the EBM compatible with the Sleep phase, we temper the EBM term in the GFlowNet reward with a schedule that decays it linearly.

C.5. Non-context-free grammar parameterization

We consider a simple extension to the context-free grammar in which the expansion rules for a NT symbol can depend on its parent. We assume a product model structure for this dependence, i.e., if P is a parent of X , then production probabilities from X – likelihoods of rules $X \rightarrow L R$ – have a form

$$p_{\theta}(L, R | X, P) \propto f_1(L, R, X; \theta) f_2(L, R, P; \theta).$$

A context-free grammar corresponds to the case of f_2 being identically 1.

We note that a generative grammar of this form with $|NT|$ nonterminal symbols can be shown to equivalent to a context-free grammar with $|NT|^2$ nonterminal symbols by a standard construction. However, directly training grammars with, e.g., 30^2 nonterminal symbols is prohibitive, while exact sampling from the posterior over parse trees in this non-context-free grammar has quintic time complexity (see Table 5).

This intractability also makes calculating the marginal likelihood difficult. As a result, we use a variational lower bound for that quantity by noting that

$$p_{\theta}(x) = \sum_z p_{\theta}(x, z) \geq \sum_{\tau \sim P_F; \tau \ni z} p_{\theta}(x, z) = F(s_0 | x) \tag{7}$$

where F is the flow estimator. Overall, we have $p_{\theta}(x) \geq F(s_0 | x)$ when the GFlowNet has converged. Thus, we use $F(s_0 | x)$, i.e., the flow of the initial state, as an estimate of a lower bound of the marginal likelihood.

C.6. Time complexity analysis

Replacing a highly optimized algorithm used for exact learning of CFGs with an amortized posterior estimator, e.g., parametrized by a Transformer, inevitably increases the run-time cost. However, there are asymptotic advantages to GFlowNet-EM compared to exact baselines, i.e., *Marginalization* and *Exact-sampling EM*.

Table 5 compares their theoretical time complexity. We use n to denote the length of input sequences and $|S|$ the number of possible symbols in z . This work focuses on presenting the method of GFlowNet-EM, and we do optimize for run time efficiency. For example, we use a Transformer with full attention, which has a time complexity of $\mathcal{O}(n^2)$ per forward pass in

Table 5. Theoretical time complexity of GFlowNet-EM and exact baselines for both the CFG and the Non-CFG we introduce as a function of n , the number of NT symbols, and $|S|$, the length of the terminal symbol sequence. GFlowNet-EM is more efficient asymptotically due to amortization. The exact baselines become intractable on the Non-CFG.

Grammar	Method	Time complexity
CFG	Marginalization Exact-sampling EM	$O(n^3 S ^3)$
	GFlowNet-EM	$O(n^2 S)$
Non-CFG	Marginalization Exact-sampling EM	$O(n^5 S ^5)$
	GFlowNet-EM	$O(n^2 S)$

Table 6. Ablation on training a GFlowNet to sample from the posterior of a fixed grammar using a variational upper bound on the marginal NLL per word. All configurations are run with 5 random seeds.

GFlowNet loss	Exploration	Sleep	NLL / word ↓
SubTB	✓	✓	$\leq 5.97 \pm 0.01$
SubTB	✓	×	$\leq 8.56 \pm 1.74$
TB	✓	×	$\leq 8.95 \pm 1.36$
TB	×	×	$\leq 9.40 \pm 1.44$
HVI	×	×	$\leq 13.14 \pm 1.55$
×	×	✓	$\leq 6.03 \pm 0.01$
Exact NLL / word			5.65

sequence length, making the complexity per trajectory $O(n^3)$, even though the theoretical complexity is just quadratic. This can be solved by simply using an architecture like a Transformer with linear attention.

C.7. Ablation studies

To understand the impact of the optimization techniques for GFlowNet-EM introduced in §4.1, we perform three ablation studies.

Effect of E-step optimization techniques. In the first study, we focus on the E-step. We fix a grammar learned with *Marginalization* to compute the reward for the GFlowNet. As the metric of comparison we use an upper bound on the negative marginal log-likelihood per word under the GFlowNet, given by $\log \frac{p_\theta(x|z)p_\theta(z)P_B(s_0 \rightarrow \dots \rightarrow z|\bar{x})}{P_F(s_0 \rightarrow \dots \rightarrow z|x)}$. The results are summarized in Table 6.

There are a few takeaways from this experiment. It is clear that a combination of all the optimization techniques is necessary for the best performance. Further, we also compare to a hierarchical VI (HVI) baseline due to its close connection with GFlowNets (Malkin et al., 2023). We observe that HVI performs the worst.

Joint learning. To understand the full impact of the techniques, we consider the full joint learning scenario in Table 8. Again, we observe that all techniques are required to get the best performance. Notably, despite strong performance on the fixed grammar, only using the Sleep phase performs much worse in the case of joint learning. This is potentially due to the fact that reward in joint learning is non-stationary and thus hard to model without exploration.

In a separate experiment, we consider the of the threshold used in the adaptive E-step. The results are summarized in Table 7. In summary, although thresholding is necessary – without it, the generative model tends to collapse, i.e., most symbols of the grammar receive almost zero mass in the posterior – if the threshold is sufficiently low, then its exact value controls the convergence rate, trading off between speed and accuracy of fitting the posterior. All thresholds result in convergence to similar final NLL and F1 scores, but we observe faster convergence to these values with higher values of the threshold.

Table 7. Ablation on training GFlowNet-EM on a context-free grammar with different threshold schedules. We vary the threshold at the start and end of training, with linear decay in between. A higher threshold results in more frequent M-steps. All configurations are run with 5 random seeds.

Threshold	NLL / word ↓	Sentence F1 ↑
12 → 6	5.77 ± 0.02	32.12 ± 2.93
8 → 4	5.78 ± 0.02	32.23 ± 3.25
6 → 3	5.76 ± 0.02	34.49 ± 2.81
4 → 2	5.79 ± 0.02	30.56 ± 4.42

Table 8. Ablations on joint learning in GFlowNet-EM for CFG. All configurations are run over 5 random seeds.

Method	NLL / word ↓	Sentence F1 ↑
GFlowNet-EM	5.70 ± 0.03	34.85 ± 3.39
-MCMC	6.02 ± 0.01	28.56 ± 0.55
-Sleep	5.91 ± 0.04	28.13 ± 0.43
-SubTB	5.84 ± 0.08	26.56 ± 7.82
-Exploration	5.70 ± 0.02	31.87 ± 1.06
Sleep Only	6.08 ± 0.06	48.41 ± 1.38

C.8. Sample parses from grammars learned by GFlowNet-EM

GFlowNet-EM is able to learn diverse tree structures for both the CFG (without EBMs) (Table 9) and the NCFG case (Table 11) but collapses to right-deep trees when guided by an EBM (Table 10). The learned latent structures that lead to better modeling of the data don’t necessarily agree with our linguistic intuition. The GFlowNet parser does not use diverse tags for top of the parse trees. This may indicate either that high-level rules are harder to learn because they depend on meaningful low-level tags, or that a greater improvement in likelihood can be achieved by better hierarchical modeling of low-level structure (e.g., having latent tags responsible for frequent bigrams). Both observations can motivate future work on more interpretable latents and better exploring the latent space using GFlowNet-EM.

D. Discrete VAE

D.1. Experiment setup

In all our experiments we use a 4×4 discrete latent representation and increase the number of categorical entries K in the dictionary from 4 to 8 to 10. We omitted larger dictionary sizes as we observed the VQ-VAE NLL worsen for $K \geq 10$. In total there are K^4 possible latent configurations.

We used a similar architecture as the one described in (van den Oord et al., 2017), adding batch normalization and additional downsizing and upsizing convolutional layers to obtain the smaller 4×4 latent representation. The GFlowNet encoder network extends the VQ-VAE convolutional image encoder by adding state encoding and state prediction MLPs. The decoder network is the same for both models. The prior distribution is modeled using a PixelCNN (van den Oord et al., 2016) with 8 masked convolution layers.

For $K = \{4, 8\}$ we trained the VQ-VAE model for 50 epochs with a learning rate of 2×10^{-4} , reduced to 5×10^{-5} at epoch 25. For $K = 10$, we trained for 80 epochs with the same learning rate, which was now reduced at epoch 50. The GFlowNet-EM + Greedy Decoder model was trained in all settings for 250 epochs, with a learning rate of 2×10^{-4} , reduced to 5×10^{-5} at epoch 180. For the experiments where the decoder is not trained with greedily-drawn samples, the training steps were doubled. Lastly, in the GFlowNet-EM + Prior experiments the models were trained for 400 epochs with similar learning rate schedules, and the reduction at epoch 300. We clarify that each GFlowNet-EM epoch is inherently slower since the encoder network requires multiple forward passes to construct the latent representation. We disabled all batch normalization layers for the GFlowNet experiments and used a batch size of 128 in all our tests.

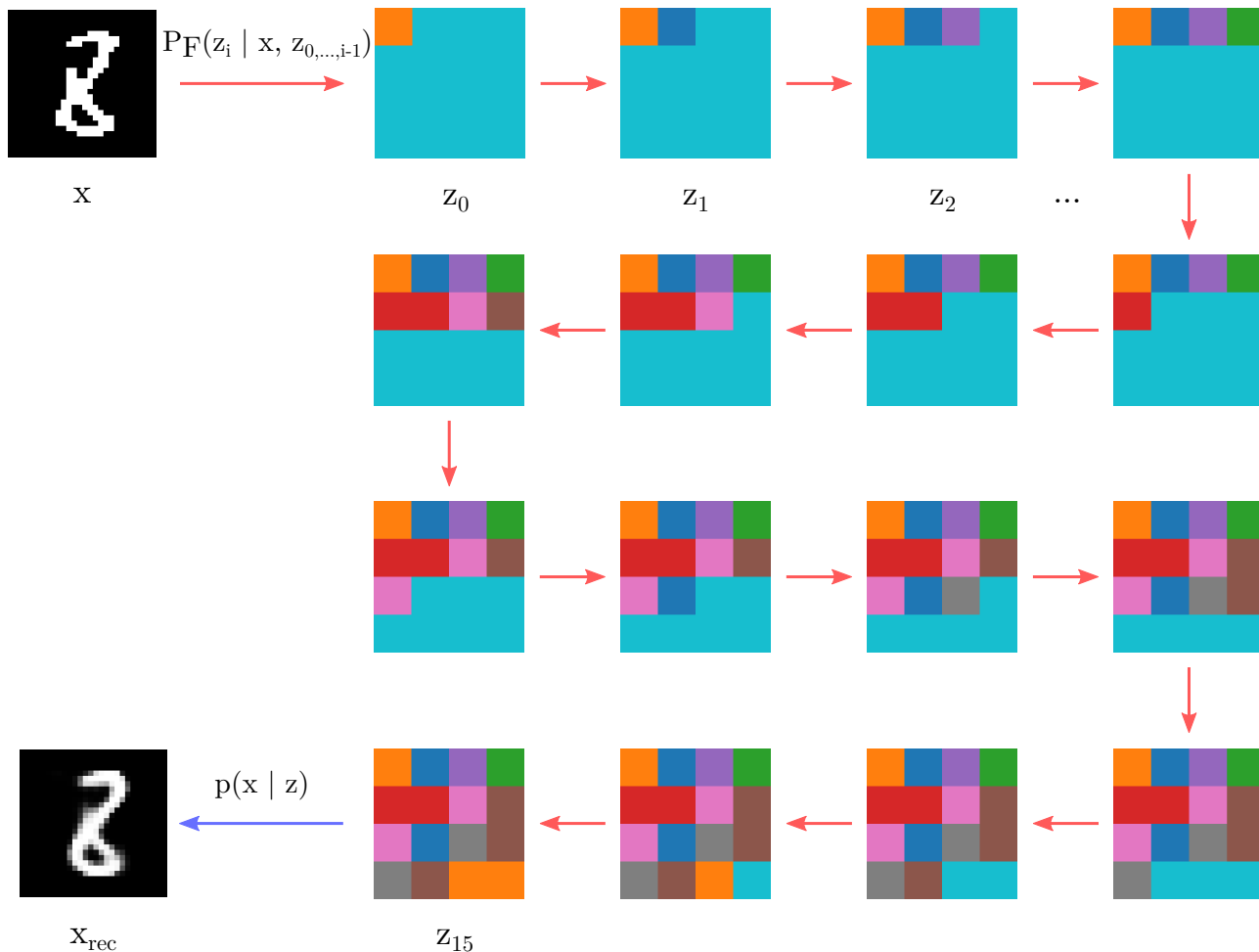


Figure 4. Visualization of the procedure of encoding an image x into a discrete representation z using a GFlowNet encoder with an autoregressive policy and reconstructing the original image.

D.2. GFlowNet-EM visualizations

In Fig. 4 we visualize the steps of encoding an input image into a discrete representation and reconstructing it. We limited the GFlowNet policy to be autoregressive, which we found to strike an appropriate balance between posterior expressiveness and model complexity. At every step the GFlowNet encoder ‘looks’ at the image and existing state and samples the next entry in the latent representation. In Figures 5 and 6 we present results of the GFlowNet-EM model with dictionary size $K = 8$ and a jointly learned prior. Despite the minimal limited latent representation, the model has captured the variety in the data which we showcase in the samples drawn from the learned prior.

E. Computation cost in practice

Grammar induction Our experiments with the context-free grammar take 23 hours to run to completion on a single V100 GPU, while the baseline from Kim et al. (2019) takes 21 hours to run on similar hardware. For completeness’ sake, we note that a specialized library called torch-struct was later developed on the basis of Kim et al. (2019)’s work, introducing several optimization tricks that reduce the computation time 8-fold. We can expect software optimizations to similarly help speed up GFlowNet-EM.

However, in the non-context-free case, a GFlowNet-EM run still takes roughly 23 hours, while exact parsing using the (generalization of) inside algorithm will take orders of magnitude longer in the absence of conditional independence assumptions. With the EBM prior on tree shape, exact parsing is completely intractable (no longer even polynomial in



Figure 5. Images from the static MNIST test set and their reconstructions using the GFlowNet-EM model with $K = 8$.

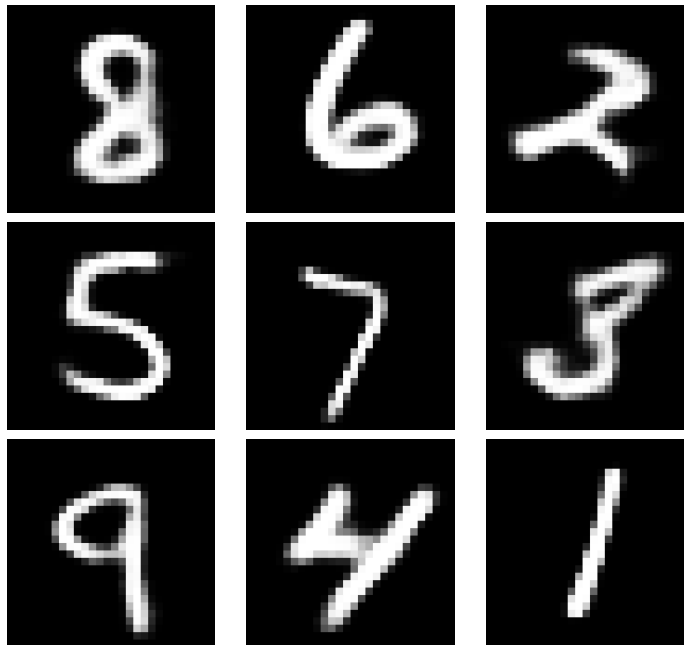


Figure 6. Samples drawn from the learned prior of the GFlowNet-EM model with dictionary size $K = 8$.

sequence length).

Discrete VAE We used a fixed number of updates for both the E and M steps. An E-step (training the GFlowNet encoder) takes approximately 25s for 400 updates, whereas the M-step (training the convolutional decoder) requires 10s for 400 updates on one A5000 GPU. In the base experiment, training takes roughly 3 hours, which is halved when the greedy decoder is used. When also learning the prior, the E and M steps take 26s and 18s respectively. Training requires again approximately 3 hours. In comparison, training any of the VQ-VAE models requires about 15m, indicating a overhead for GFlowNet-EM with greedy decoder training. Future work should consider ways to accelerate GFlowNet-EM training, such as by better selection of learning rates and update schedules for the E, sleep, and M steps, which we did not extensively tune for the experiments in this paper.

Table 9. Sample parses generated with GFlowNet-EM on a context-free grammar.

Parse Tree	$\log Z(x)$	$\log p(z x)$
<p>A parse tree for the sentence "portrait studios have also junk_i". The root node is Q15, which branches into Q15 and junk_i. The left Q15 branches into Q15 and Q7. The left Q15 branches into Q14, which branches into portrait and studios. The Q7 node branches into have and also.</p>	-43.68	-49.19
<p>A parse tree for the sentence "but around it began had fallen then as quickly the dow". The root node is Q15, which branches into Q15 and around. The left Q15 branches into but and Q15. The right Q15 branches into Q15 and Q18. The right Q18 branches into to and turn. The left Q15 branches into Q15 and Q23. The right Q23 branches into it and began. The left Q15 branches into Q15 and Q22. The right Q22 branches into had and fallen. The left Q15 branches into Q15 and Q3. The right Q3 branches into as and Q12. The right Q12 branches into the and dow. The left Q15 branches into then and Q4. The right Q4 branches into as and quickly.</p>	-112.76	-126.26
<p>A parse tree for the sentence "to make them directly comparable each index is based on the close of N equaling N". The root node is Q28, which branches into Q28 and Q9. The right Q9 branches into equaling and N. The left Q28 branches into Q28 and Q22. The right Q22 branches into on and Q11. The right Q11 branches into the and close. The left Q28 branches into Q28 and Q13. The right Q13 branches into Q27 and Q13. The right Q13 branches into each and index. The left Q28 branches into Q10 and Q13. The right Q13 branches into Q13. The right Q13 branches into is and based. The left Q10 branches into Q3 and them. The right Q3 branches into to and make. The left Q13 branches into Q6 and Q13. The right Q13 branches into directly and comparable.</p>	-85.03	-94.73

Table 10. Sample parses generated with GFlowNet-EM on a context-free grammar with an annealed EBM prior.

Parse	$\log Z(x)$	$\log p(z x)$
<p>A parse tree for the sentence "this market has been very badly damaged". The root node is Q3, which branches into "this" and Q25. Q25 branches into "market" and Q14. Q14 branches into "has" and Q25. This Q25 branches into "been" and Q25. The final Q25 branches into "very", and the final Q25 branches into "badly" and "damaged".</p>	-48.21	-51.02
<p>A parse tree for the sentence "u.s. treasury bonds were higher in overnight trading in japan which opened at about 11:00 p.m. edt". The root node is Q3, which branches into "u.s." and Q25. Q25 branches into "treasury" and Q25. This Q25 branches into "bonds" and Q14. Q14 branches into "were" and Q13. Q13 branches into "higher" and Q14. This Q14 branches into "in" and Q3. This Q3 branches into "overnight" and Q25. This Q25 branches into "trading" and Q14. This Q14 branches into "in" and Q3. This Q3 branches into "japan" and Q14. This Q14 branches into "which" and Q14. This Q14 branches into "opened" and Q14. This Q14 branches into "at" and Q3. This Q3 branches into "about" and Q3. This Q3 branches into "N:N" and Q25. The final Q25 branches into "p.m." and "edt".</p>	-118.52	-114.69
<p>A parse tree for the sentence "to make them directly comparable each index is based on the close of N equaling N". The root node is Q3, which branches into "to" and Q25. Q25 branches into "make" and Q3. This Q3 branches into "them" and Q14. Q14 branches into "directly" and Q25. This Q25 branches into "comparable" and Q3. This Q3 branches into "each" and Q25. This Q25 branches into "index" and Q14. This Q14 branches into "is" and Q25. This Q25 branches into "based" and Q14. This Q14 branches into "on" and Q3. This Q3 branches into "the" and Q25. This Q25 branches into "close" and Q14. This Q14 branches into "of" and Q23. This Q23 branches into "N" and Q12. The final Q12 branches into "equaling" and "N".</p>	-94.38	-96.89

Table 11. Sample parses generated with GFlowNet-EM on a non-context-free grammar.

Parse	$\log Z(x)$	$\log p(z x)$
<p>A parse tree for the sentence "portraits studios have also junk onto the trend". The root node is Q9, which branches into "portraits" and another Q9 node. This second Q9 node branches into "studios" and another Q9 node. This third Q9 node branches into Q25 and Q5. The first Q25 node branches into another Q25 and "junk". The second Q25 node branches into "have" and "also". The Q5 node branches into "onto" and Q11. The Q11 node branches into "the" and "trend".</p>	-42.11	-50.74
<p>A parse tree for the sentence "but then as quickly as the dow had fallen it began to turn around". The root node is Q9, which branches into Q11 and another Q9 node. The Q11 node branches into "but" and "then". The second Q9 node branches into Q16 and another Q9 node. The Q16 node branches into "as" and "quickly". The third Q9 node branches into Q25 and Q5. The first Q25 node branches into "as" and Q11. The Q11 node branches into "the" and "dow". The second Q25 node branches into "had" and "fallen". The Q5 node branches into Q25 and another Q5. The first Q25 node branches into "it" and Q28. The Q28 node branches into Q10 and "turn". The Q10 node branches into "began" and "to". The second Q5 node branches into "around".</p>	-117.60	-153.98
<p>A parse tree for the sentence "to make them directly comparable each index is based on the close of N equaling N". The root node is Q17, which branches into Q7 and another Q17 node. The Q7 node branches into Q27 and "them". The Q27 node branches into "to" and "make". The second Q17 node branches into Q3 and another Q17 node. The Q3 node branches into "directly" and Q12. The Q12 node branches into "comparable" and "each". The third Q17 node branches into "index" and another Q17 node. The fourth Q17 node branches into Q15 and Q10. The first Q15 node branches into "is" and "based". The second Q15 node branches into Q12 and Q20. The Q12 node branches into "on" and Q7. The Q7 node branches into "the" and "close". The Q20 node branches into "of" and "N". The Q10 node branches into "equaling" and "N".</p>	-91.77	-105.96